The *tat* Gene of Human T-Lymphotropic Virus Type 1 Induces Mesenchymal Tumors in Transgenic Mice

MICHAEL NERENBERG, STEVEN H. HINRICHS, R. KAY REYNOLDS, GEORGE KHOURY, GILBERT JAY*

Human T-lymphotropic virus type 1 (HTLV-1) is a suspected causative agent of adult T-cell leukemia. One of the viral genes encodes a protein (tat) that not only results in transactivation of viral gene expression but may also regulate the expression of certain cellular genes that are important for cell growth. Transgenic mice that expressed the authentic tat protein under the control of the HTLV-1 long terminal repeat were generated, and cell types that are permissive for the viral promoter and the effects of the *tat* gene on these cells were studied. Three of eight founder mice with high levels of expression of the transgene in muscle were bred and then analyzed. All developed soft tissue tumors at multiple sites between 13 to 17 weeks of age. This phenotype was transmitted to nine of nine offspring that inherited the *tat* gene and were available for analysis. The remaining five founders expressed the transgene in the thymus, as well as in muscle. This second group of mice all exhibited extensive thymic depletion and growth retardation; in all of these mice, death occurred between 3 to 6 weeks of age before tumors became macroscopically visible. The *tat* gene under the control of the HTLV-1 regulatory region showed tissue-specific expression and the tat protein efficiently induced mesenchymal tumors. The data establish tat as an oncogenic protein and HTLV-1 as a transforming virus.

HUMAN T-LYMPHOTROPIC VIRUS TYPE 1 (HTLV-1) HAS been associated with an adult form of T-cell leukemia (*1*). This malignancy is derived from a monoclonal proliferation of CD4-positive T cells (*2*). Despite epidemiologic evidence, it has been difficult to establish a clear role for HTLV-1 in the genesis of this form of leukemia.

Current data are consistent with HTLV-1 being required but insufficient by itself to induce adult T-cell leukemia (ATL). Less than 0.1 percent of individuals infected by the virus ever develop the disease (*3*). Malignancy develops after a characteristically long latent period of as many as 20 years after initial exposure (*4*). Even more complex is the finding that fresh isolates of peripheral leukemic cells frequently do not have detectable viral antigens (*5*). Together, these observations suggest that an independent second event is required subsequent to the action of HTLV-1 in order to induce ATL. The HTLV-1 may function to initiate the process that ultimately leads to the development of the disease. However, after this initiation function is achieved, viral products are not required for the maintenance of the malignant phenotype. This proposed mechanism for the role of HTLV-1 in the disease process is difficult to study in vitro and, therefore, an animal model is needed in order to delineate the role of this particular infectious agent.

Epidemiologic studies suggest that HTLV-1 is a poorly transmitted agent, and its mode of infection is not well understood. Infections in vitro are difficult to obtain and occur only after prolonged co-cultivation with other cells by the agglutination of these cells to form syncytia (*6*). In vitro transmission of the virus by cell fusion is not restricted to T cells. Cells of lymphoid, endothelial, fibroblastic, osteoid, and muscle origin have been successfully infected in this manner (*7*). However, immortalization by HTLV-1 is only known for T cells (*8*). Although other syndromes, such as the occurrence of central nervous system disease (*9*) and hypercalcemia (*10*), have been reported among HTLV-1–infected individuals, they have not been extensively studied.

Apart from the structural genes (*gag*, *pol*, and *env*) normally carried by nondefective retroviruses, the genome of HTLV-1 contains a region that encodes three distinct and overlapping proteins, designated $p40^x$, $p27^x$, and $p21^x$ (*11, 12*). The best studied of these is $p40^x$, a 40-kD protein encoded by a 2-kb doubly spliced messenger RNA (mRNA) (*13*). In vitro studies have shown that this gene product, which has generally been referred to as the tat protein, is capable of transactivating the HTLV-1 long terminal repeat (LTR) (*14*), the transcriptional regulatory region of the virus. Because of its role in stimulating viral gene expression and the suggestion that the tat protein encoded by HTLV-1 and HTLV-2 may also regulate the expression of certain cellular genes (*15*), it seems probable that the tat protein may act to alter the growth of infected cells.

Malignancies induced by retroviruses occur via two general mechanisms (*16*). (i) Slowly transforming retroviruses induce tumors after a long latency period by integration at specific chromosomal sites which lead to the aberrant activation of adjacent cellular genes (*17*). (ii) Retroviruses that transform cells relatively quickly induce malignancies rapidly through a series of events initiated by the product of the viral oncogene, which frequently has homology to a cellular gene. HTLV-1 appears to have features of both types of

The authors are in the Laboratory of Molecular Virology, National Cancer Institute, Bethesda, MD 20892.

*To whom correspondence should be addressed at National Cancer Institute, Building 41, Room A101, Bethesda, MD 20892.

viruses. Whereas there are several nonstructural viral genes that could serve as oncogenes, there is also a characteristic long latency prior to the development of ATL. There has been no association of malignancy with site-specific viral integration (*18*) or evidence for the existence of a human cellular homolog to any of the nonstructural viral genes (*19*). However, homology to an endogenous mouse gene has been suggested (*20*).

In view of the inherent difficulties in studying this virus by conventional means, we developed a transgenic mouse model to further define the role of the *tat* gene under the control of the HTLV-1 LTR.

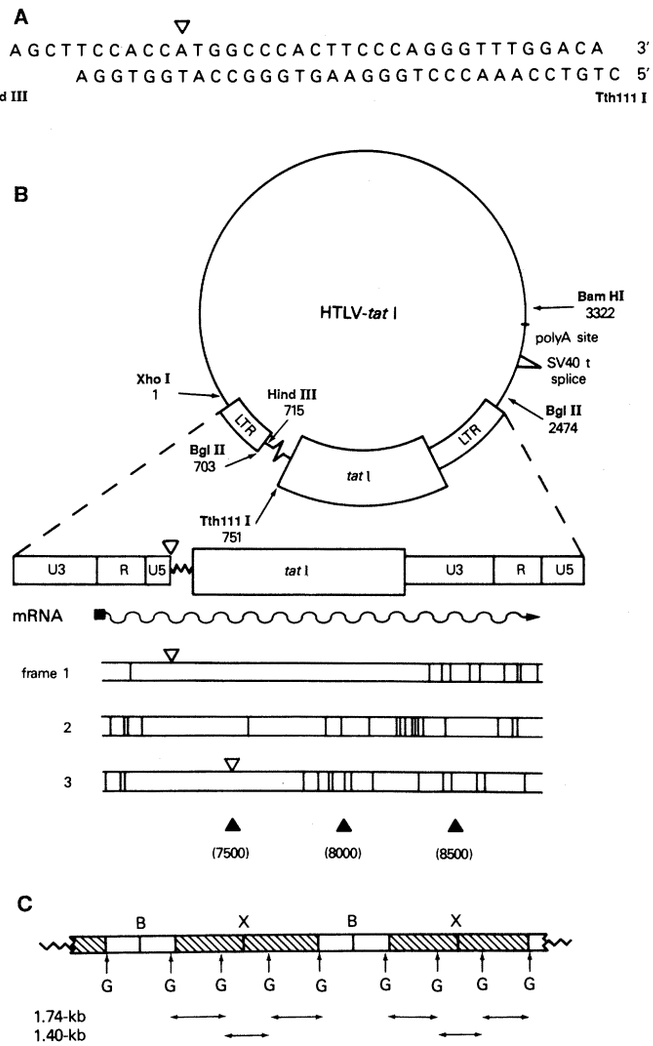

Fig. 1. Features of the HTLV-*tat*1 plasmid. (**A**) Sequence of the two complementary strands of the synthetic oligonucleotide linker, showing the 5′ Hind III and 3′ Tth111 I cloning sites. The upper strand contains the methionine initiation codon (▽), flanked by the Kozak consensus sequence (CCACCATGG) (*22*), and eight other codons that encode the amino terminus of the tat1 protein. (**B**) Plasmid HTLV-*tat*1. The 5′ and 3′ viral LTRs are represented by the small boxes. The tat1 coding sequence is shown by the large box. The zigzag line indicates the location of the synthetic oligonucleotide linker. The numbers represent nucleotide positions starting from the Xho I site. The entire plasmid is 6191 bp. At the bottom is an expanded view of the entire transcriptional unit. The 5′ LTR contains a partial deletion of U5. The wavy line indicates the corresponding transcribed mRNA. In the analysis of open reading frames, the vertical lines represent termination codons. The numbers in parentheses correspond to those described by Seiki *et al.* (*18*) for the proviral sequence. (**C**) Hypothetical integration pattern of the injected DNA fragment, based on the assumption of head-to-head and tail-to-tail ligation in vivo. The restriction sites shown are Bam HI (B), Xho I (X), and Bgl II (G). The expected hybridizing fragments, generated by Bgl II digestion and detected by DNA blot analysis with a DNA probe homologous to the shaded region, are indicated (arrows).

Construction of a LTR-*tat*1 expression vector. The *tat* gene product has been shown to transactivate the HTLV-1 LTR and high level expression of the tat protein may be achieved by placing the HTLV-1 LTR immediately upstream of the tat coding sequence (*14*). To generate such a chimeric construct, we have used a proviral LTR sequence that contains the U3, R, and part of the U5 region (*14*), and a separate proviral DNA segment which includes an almost complete *tat* coding sequence (*21*). The latter fragment begins with the Tth111 I site at codon position 9 and extends beyond the termination codon to the end of the 3′ proviral LTR (Fig. 1). These two fragments were joined by a synthetic duplex designed to incorporate several convenient features (Fig. 1A). At the 5′ and 3′ ends were placed the unidirectional cloning sites, Hind III and Tth111 I, respectively. This oligonucleotide reconstituted the initiation codon normally provided by the *env* gene, as well as the next eight codons of the *tat* mRNA. To ensure efficient translation of the mRNA, we retained the eukaryotic translational consensus sequence (CCACCATGG) (*22*) at the 5′ side of the coding region. This construct, designated HTLV-*tat*1, should encode an authentic tat protein, identical to that derived from the doubly spliced mRNA.

Transcription of the HTLV-*tat*1 construct is expected to initiate at the beginning of the R region in the 5′ LTR, proceed across the tat coding sequence and terminate toward the end of the R region in the 3′ LTR (Fig. 1B). Downstream of the 3′ LTR, our construct includes the SV40 small-t splice site and the SV40 early polyadenylation [poly(A)] site in tandem because the spliced mRNA may be more stable. If transcriptional 3′ processing occurs at the SV40 poly(A) site rather than at the 3′ LTR R region, splicing within the SV40 segment is expected. Transfection experiments in vitro have confirmed that the HTLV-*tat*1 construct encodes predominantly an approximately 2-kb transcript, initiating at the appropriate cap site within the 5′ LTR and terminating at the poly(A) site within the 3′ LTR.

Analysis of the various translational reading frames of the tat mRNA derived from the HTLV-*tat*1 construct revealed not only a long open reading frame (frame 1), with an appropriate initiation codon that would encode the 40-kD tat or $p40^x$ protein, but also several shorter open reading frames (Fig. 1B). Reading frame 3 would normally encode $p27^x$ and $p21^x$ (*11*); however, the former will not be expressed in this case because of the lack of an appropriate initiation codon. The initiation codon for $p21^x$ is the second in this construct, but is located far downstream from that of tat and is preceded by a pentanucleotide that does not conform to the preferred consensus translational initiation sequence. Therefore, it would not be expected to be translated efficiently. Previous studies with HTLV-1 infected cells show a very low level of accumulation of this protein (*12*). Transfection experiments in vitro have confirmed that the HTLV-*tat*1 construct encodes the authentic 40-kD tat protein capable of transactivating an LTR chloramphenicol acetyltransferase test gene (*cat*).

Production and screening of transgenic mice. To facilitate integration and efficient expression in target tissues, we excised the entire tat transcriptional unit from HTLV-*tat*1 from all bacterial plasmid sequences by combined cleavage with Xho I and Bam HI (Fig. 1). The purified DNA fragment was microinjected into fertilized eggs from superovulated CD-1 females, which are outbred mice (Jackson Laboratory) that were mated with (C57BL/6 × DBA/2)F_1 males. Six litters, each with two to seven offspring, were produced. Genomic DNA from the tail tissue of each mouse was digested with Bgl II, which cuts twice within the injected fragment and releases virtually the entire transcribed region of the *tat* gene.

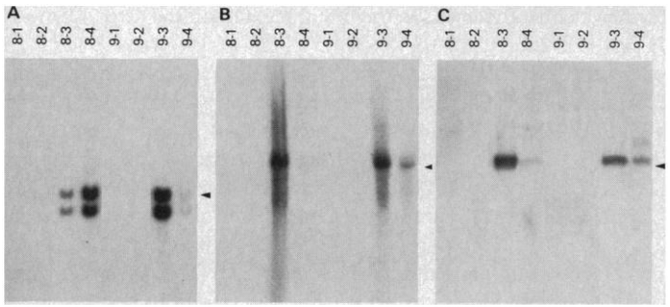

Fig. 2. Screening for transgenic mice; analyses of representative mice from litters 8 and 9. (**A**) DNA blot analysis. Tail DNA (20 μg) was digested with Bgl II, fractionated on a 1 percent agarose gel, and transferred to a nitrocellulose membrane (*26*). Hybridization was performed with an M13 DNA probe containing LTR and *tat* sequences. The arrowhead identifies the 1.74-kb fragment, which represents intact copies of the transgene. (**B**) RNA blot analysis. Tail RNA (15 μg), obtained by the isothiocyanate–cesium chloride procedure, was fractionated on a 1 percent agarose-formaldehyde gel and transferred to a nitrocellulose membrane (*27*). Hybridization was performed with the same DNA probe described above. The arrowhead indicates the position of the 2-kb transcript. (**C**) Protein immunoblot analysis. Tail protein (40 μg), obtained by homogenization of tissues in 2 percent SDS and 5 percent β-mercaptoethanol, was fractionated on a 10 percent polyacrylamide-SDS gel and transferred to a nitrocellulose membrane (*28*). The blot was probed with a 1 to 100 dilution of an antibody to a tat fusion protein. The arrowhead identifies the position of the 40-kD tat protein.

The presence of this 1.74-kb fragment in the genomic DNA digest, as revealed by DNA blot analysis, would indicate the integration of at least one intact copy of the transgene. Since the injected DNA fragment was derived by digestion with two different enzymes, Xho I and Bam HI, head-to-head and tail-to-tail oligomerization may occur before integration. Digestion of tail DNA with Bgl II would produce a 1.74- and a 1.40-kb fragment detected by hybridization with a ^{32}P-labeled single-stranded DNA probe which include LTR and tat sequences (Fig. 1C).

The DNA from animals 8-1, 8-2, 9-1, and 9-2 showed no hybridization, but DNA from 8-3, 8-4, 9-3, and 9-4 contained the two characteristic components confirming the presence of intact copies of the transgene (Fig. 2A). The extent of hybridization varied among the transgenic mice. If we assume that these mice are not mosaic, this observation indicates the presence of varying numbers of copies of the transgene in different individuals. Prolonged exposure of the DNA blots also revealed differing flanking sequences, an observation that is consistent with the lack of a specific integration site for the *tat* gene within the mouse genome.

Of the 28 offspring generated, 10 (about 35 percent) were positive for tat sequences (Fig. 3). We first analyzed tissue extracts from the tails of these mice for the expression of the integrated *tat* gene. RNA blot analysis revealed a single major component of about 2-kb in size in all of the transgenic mice, including animals 8-3, 8-4, 9-3, and 9-4 (Fig. 2B). While most of these mice showed a high level of tat transcripts in their tails, mouse 9-4 expressed somewhat less and mouse 8-4 much less steady-state mRNA. This variation in mRNA expression did not correlate with the presence of varying copies of the transgene (Fig. 2A). Mouse 8-3 with a lower number of the *tat* gene expressed abundant mRNA and mouse 8-4 with a high copy number expressed barely detectable amounts of mRNA. Protein blot analysis with a rabbit polyclonal antiserum to a bacterially expressed tat fusion protein revealed the presence of a 40-kD component in the tail lysates of all the transgenic mice but not in their normal littermates (Fig. 2C). Expression of the 40-kD protein correlated well with expression of the 2-kb transcript (Fig. 2, B and C). Analysis of RNA and protein from the other founders revealed levels intermediate between those of animals 8-3 and 9-4. This observation suggests, but does not prove, that expression of the transgenic *tat* gene may be controlled at the transcriptional level.

Transgenic mice that are slow-growing express tat in thymus and die with thymic involution. One of the ten transgenic mice (designated 5-5) died 1 day after birth, presumably for reasons not related to the presence of the *tat* gene. The remaining nine transgenic mice were phenotypically indistinguishable from their normal littermates at the time of birth. However, by 10 to 14 days of age, five of these mice (5-1, 7-1, 8-3, 9-3, and 10-1), each from a different litter, were growing more slowly than their littermates. This difference was obvious by 3 weeks of age, at which time these mice were about half the weight of others in the litter. These mice died between 3 to 6 weeks of age. Since none of these mice reached sexual maturity, the lines could not be propagated.

Autopsies on all five small mice showed extensive involution of the thymus (Fig. 4). The normal thymus has a thick and highly cellular cortex surrounding a less cellular medulla (Fig. 4A). The sharpness of the corticomedullary junction is accentuated by this difference in cellularity (Fig. 4C), in sharp contrast to the thymus of the tat-positive mouse which shows a disproportionate thinning of the cortex (Fig. 4B). In addition, the hypocellularity observed in the cortex was accompanied by blurring of the corticomedullary junction (Fig. 4D). This was seen in all transgenic mice that were slow-growing and died, and from which thymic remnants could be identified at autopsy. Microscopic analysis of the lungs from these mice yielded evidence of pneumonia, suggesting that secondary infections may have been the cause of death.

In order to support the idea that expression of the tat protein is responsible for thymic depletion, we analyzed the expression of the transgene in different tissues from these deceased mice. Our finding that all transgenic mice, with either the small or the large phenotype, expressed the tat protein in their tails is not definitive of cell origin because the tail is extremely complex and contains muscle, nerve, skin, fibrous tissue, cartilage, bone, and marrow. Protein immunoblot analysis of various tissues from mice with the lethal phenotype showed an extremely high level of the tat protein in muscle, less in

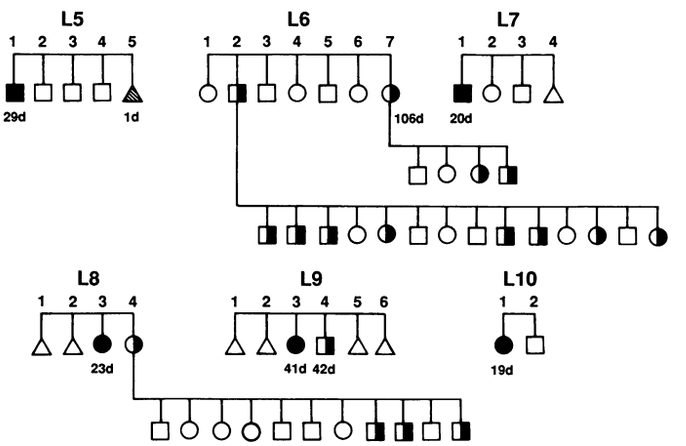

Fig. 3. Pedigree analysis. Six litters of mice (designated L5 through L10) were generated by implanting fertilized eggs that were microinjected with approximately 100 copies of the LTR-*tat* gene into pseudopregnant females (*29*). Of the 28 offspring obtained, 10 were found positive for tat1 sequences. Except for mouse 5-5 (designated ▲), which died 1 day after birth, the remaining nine transgenic mice exhibited either a small (designated ■ or ●) or a normal (designated ◨ or ◑) size phenotype. Mice with the small phenotype (5-1, 7-1, 8-3, 9-3, and 10-1) did not reach maturity to breed, and all died at the indicated age of thymic involution. Mice with the normal size phenotype (6-2, 6-7, 8-4, and 9-4) all developed tumors and three of them were successfully bred with CD-1 females or C57BL/6 males to generate positive F_1 mice. The sex of the mice is as indicated: □, male; ○, female; △, undetermined.

the thymus and stomach, and only traces in most other tissues (Fig. 5A). While the high level of expression in muscle may explain our detection of small amounts of the tat protein in most tissues, it cannot account for expression in the thymus. The expression in the thymus has been greatly underestimated because this organ was highly atrophied at the time of analysis. Indeed, mouse 5-5, which died 1 day after birth, showed comparable expression of the *tat* gene in the thymus and in muscle. Together, these results suggest preferential expression of the LTR-*tat* gene in muscle and thymus, both of which contain mesenchyma. The expression in the thymus may be responsible for the observed thymic phenotype.

Transgenic mice of normal size phenotype do not express tat in thymus and develop mesenchymal tumors. The remaining transgenic mice (6-2, 6-7, 8-4, and 9-4) were all indistinguishable in size from their normal littermates. Except for mouse 9-4, which died of unknown cause 42 days after birth, all transgenic mice in this group reached maturity and were able to breed. All three founders eventually developed soft tissue tumors. In the two founders with high levels of expression of the tat protein in tail, these tumors occurred within a week of each other at 90 (6-7) and 97 (6-2) days of age. The third founder (8-4), which showed significantly less tail expression of the *tat* gene and was mosaic for this gene, developed tumors at 120 days of age. In all three founders, the tumors were multicentric, with simultaneous nodules arising most commonly on the ear, nose, mouth, foot, and tail (Fig. 6A). Tumors were obtained for microscopic analyses either surgically, with the mouse under anesthesia (6-2, 8-4), or at time of death (6-7). Prominent features include a spindle-shaped cell morphology characteristic of tumors of mesenchymal derivation, with frequent infiltration by granulocytes (Fig. 6B); expression of the tat protein in all tumors analyzed was higher than that in any other tissue. Many of the tumors were slow-growing, but those that grew rapidly showed a high mitotic index, which is indicative of a malignant phenotype (Fig. 6C). There was no evidence of hematogenous or lymphatic spread.

Mouse 6-7 developed a fast-growing submandibular tumor at 90 days of age, shortly after giving birth to her first litter. All members of the litter died soon after birth; and mouse 6-7 died at 106 days of age. We were, therefore, unable to maintain this transgenic line. Mouse 6-2, a transgenic male, was able to mate and had 14 progeny, of which 8 inherited the *tat* gene. Except for one mouse, which was killed at an early age for the analysis of the expression of the tat protein in different tissues, all positive F_1 mice from this litter developed tumors. None of the normal littermates showed a similar phenotype. Mouse 8-4 transmitted the *tat* gene to 3 of 11 offspring in the first litter. One was killed for the analysis of tissue-specific expression and the remaining two both developed tumors. Again, all of their normal littermates remained free of tumors.

To explain the phenotype of this second group of transgenic mice, we analyzed the expression of the *tat* gene in F_1 mice before they developed their tumor phenotype. Immunoblot analysis revealed a high level of expression of the tat protein only in muscle of both 6-2 and 8-4 mouse lines. While 6-2 progeny also expressed a low level of the tat protein in the bladder (Fig. 5B), 8-4 progeny expressed low but detectable amounts in several other tissues. This restricted

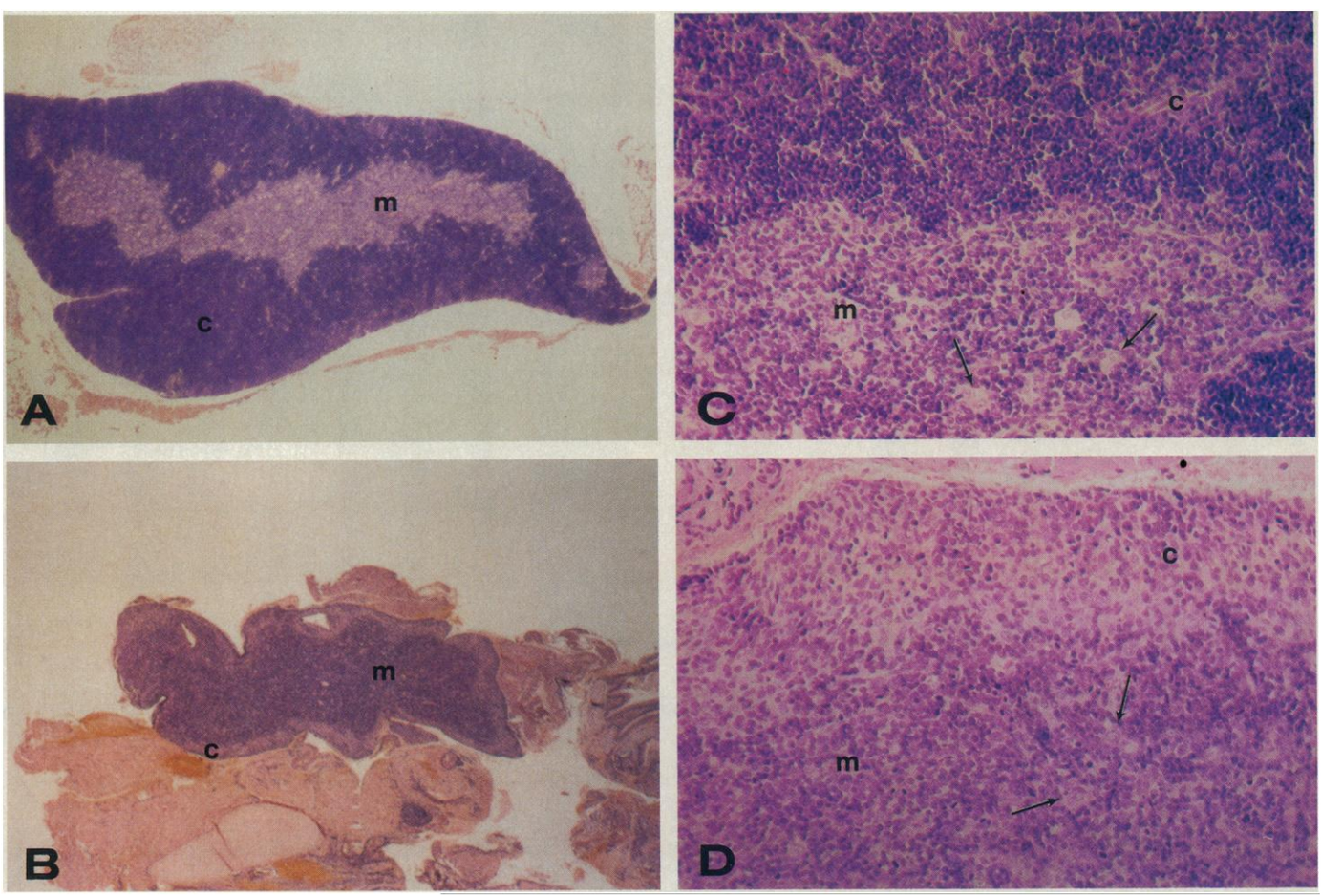

Fig. 4. Microscopic examination of the thymus. A tat-negative mouse (7-3) (**A** and **C**) and a tat-positive mouse (7-1) (**B** and **D**), both from the same litter, were killed at 21 days of age. Paraffin-embedded sections of the thymuses, stained by hematoxylin and eosin, were compared microscopically at ×25 (A and B) and ×160 (C and D) magnification. The arrows indicate epithelioid cells in the medulla; c, cortex. m, medulla.

distribution of the tat protein may explain the type of tumors that arise later in life. The complete lack of expression in the thymus of both 6-2 and 8-4 mice correlated with the absence of any thymic abnormality and suggests that the thymic depletion observed in the first group of transgenic mice may be the result of the expression of the *tat* gene in that tissue.

Correlation of tat expression with disease in transgenic mice. The low ratio of disease to HTLV-1 infection and the lack of correlation of viral gene expression with maintenance of the disease (*3*) have raised questions regarding the role of HTLV-1 in malignancy. Our study establishes the *tat* gene as oncogenic.

In vitro studies have suggested that the virus has no significant tissue restriction (*23*). Since the virus is carried and circulated by T cells, contact with most tissues in the body would be expected. Nevertheless, clinical data regarding disease other than lymphoid malignancies have only recently been accumulated (*9, 10*).

To permit a systematic approach to studying the pathogenetic role of the *tat* gene, we considered it crucial to develop an animal model. By deriving transgenic mice in which the *tat* gene was controlled by its own natural promoter, the expression of this gene in all permissive cell types was allowed and the variability inherent in viral infections was circumvented. In these mice, expression of the *tat* gene was found in a variety of tissues. While expression in muscle was high in every founder mouse, some but not all also expressed significant amounts in thymus. The reason for the apparent difference in thymus expression of the tat protein in the two sets of mice is not clear. It cannot be the result of random integration of the transgene at chromosomal sites which affect its expression, because multiple founder mice were derived for each of the two phenotypes even in the same litter. It is possible, however, that specific integration in multiple, preferred chromosomal regions may give rise to one or the other phenotype. At present, we do not know what specific cell types in the thymus and in muscle express the transgene. However, it does appear that the HTLV-1 LTR is not equally expressed in all tissue types in vivo, as suggested by transfection studies in vitro (*23*).

Two distinct phenotypes were associated with the expression of the tat protein in these transgenic mice. All founders that expressed the transgene in the thymus developed extensive thymic atrophy early in life. At the cellular level, the depletion is particularly severe in the cortex. This phenotype was accompanied by progressive growth retardation and eventual death at about 3 to 4 weeks of age. Since these mice do not mature to breed, all further experiments directed at the mechanism for thymic depletion will have to be performed on newly derived transgenic mice.

Although the exact link between thymic hypoplasia and growth retardation has not been established, this correlation has been

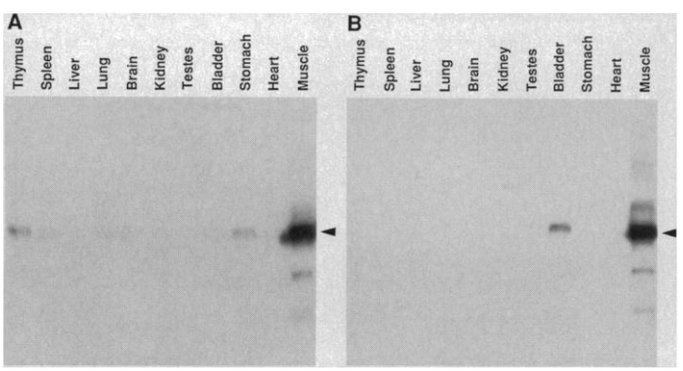

Fig. 5. Tissue distribution of the tat protein in transgenic mice. Equivalent amounts of total protein, obtained from different tissues by boiling in 2 percent SDS and 5 percent β-mercaptoethanol, were fractionated on a 10 percent polyacrylamide-SDS gel and transferred to a nitrocellulose membrane (*28*). The blot was probed with a 1 to 100 dilution of an antibody to a tat fusion protein (*29*). The arrowheads indicate the positions of the 40-kD tat protein. (**A**) Mouse 7-1 with the small phenotype. (**B**) F_1 mouse from 6-2 with a normal size phenotype.

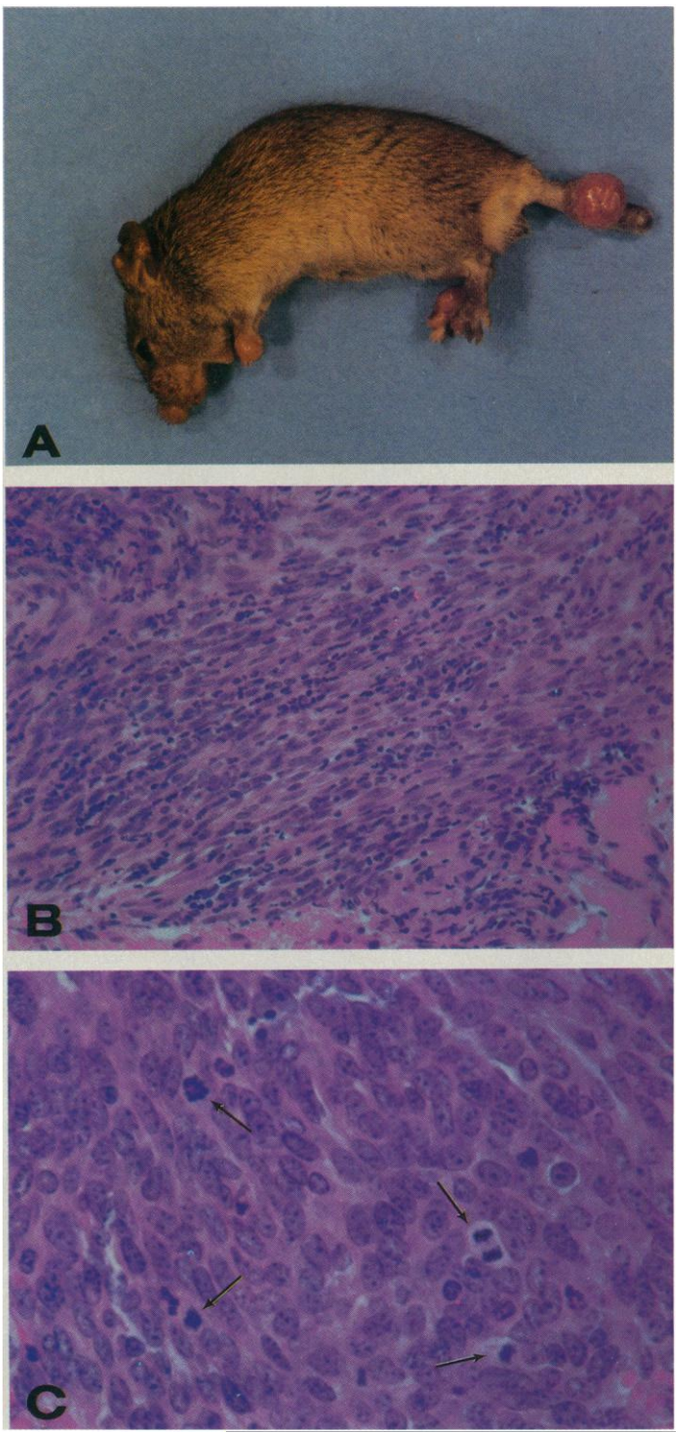

Fig. 6. Tumors from mice with the normal size phenotype. (**A**) F_1 mouse from 6-2, with multiple tumors growing simultaneously on the nose, ears, feet, and tail. (**B**) Paraffin-embedded section of a tumor from one of the ears showing typical spindle-shaped cells with infiltrating polymorphonuclear leukocytes and surrounding mesenchymal tissue. Hematoxylin and eosin stained and photographed at ×160 magnification. (**C**) Section of a fast-growing tumor from the tail showing elongated tumor cells with a high nuclear to cytoplasmic ratio and multiple mitotic figures (arrows). Hematoxylin and eosin stained and photographed at ×400 magnification.

observed in studies where the thymus has been damaged by extrinsic factors (*24*). In our studies of the small phenotype mice, growth retardation and thymic atrophy may have resulted from secondary systemic effects. However, this effect seemed to be specific since no spontaneous runting in control mice was seen in our study. In all five instances, growth retardation was associated with tat expression in the thymus. In humans, HTLV-1 is generally not transmitted vertically and the infection usually does not occur until after both maturation of the immune system and thymic atrophy have occurred. Thymic involvement in ATL has, therefore, not been observed.

The transgenic mice that did not express the tat protein in the thymus all developed mesenchymal tumors between 13 and 17 weeks of age. This occurred regardless of whether these mice were back-crossed to C57BL/6 or to CD-1 mice. These have now been identified as neurofibromas (*25*).

Analysis of DNA from mice that bear tumors provides no evidence of site-specific integration. Since every tumor that has been analyzed expressed a high level of the tat protein and since mice with lower expression of this protein showed later onset of the disease, it seems likely that the *tat* gene product is responsible, directly or indirectly, for this phenotype. An example of the latter would be activation of endogenous or exogenous viruses. While transgenic mice with the atrophic thymus phenotype also expressed the *tat* gene product in muscle, none of the five mice showed obvious signs of tumor growth at the macroscopic level. This is probably due to the death of these five mice at an early age (usually between 3 to 6 weeks old) before the development of the tumor phenotype, which is not apparent until a much later age (usually between 13 to 17 weeks old). Retrospective analysis of mouse 9-3, which died at a somewhat later stage of development (about 7 weeks) than others with the small phenotype, supports this contention. Microscopic analysis revealed multiple tumor nodules that were not perceptible by gross examination.

Our study establishes that expression of the tat protein in appropriate cell types induces tumors in mice. It is unlikely that an independent mutational event, in conjunction with the expression of the tat protein, is required to manifest the observed phenotype, because multiple simultaneous independent tumors arose in all of the animals. It may well be that expression of the tat protein in the appropriate target tissues is sufficient to perturb normal cellular functions and to cause the disease. However, the appearance of histologic changes in a few of the rapidly growing tumors may reflect a separate event.

While a cellular homolog of the viral *tat* gene has not been identified in humans, the definition of an oncogene as a gene involved in perturbing normal cellular functions leading to malignancy (*15*) would appear to include *tat*. Thus, HTLV-1 should be reevaluated as a transforming retrovirus.

REFERENCES AND NOTES

1. B. J. Poiesz *et al.*, *Proc. Natl. Acad. Sci. U.S.A.* 77, 7415 (1980); M. Yoshida, I. Miyoshi, Y. Hinuma, *ibid.* **79**, 2031 (1982); Y. Hinuma *et al.*, *ibid.* **78**, 6476 (1981); V. S. Kalyanaraman *et al.*, *ibid.* **79**, 1653 (1982); M. Robert-Guroff *et al.*, *Science* **215**, 975 (1982); R. Weiss, in *RNA Tumor Viruses,* R. Weiss, N. Teich, H. Varmus, J. Coffin, Eds. (Cold Spring Harbor Laboratory, Cold Spring Harbor, NY, 1982), pp. 1205–1281.
2. B. J. Poiesz, F. W. Ruscetti, M. S. Reitz, V. S. Kalyanaraman, R. C. Gallo, *Nature (London)* **294**, 268 (1981); I. Miyoshi *et al.*, *ibid.*, p. 770; N. Yamamoto, M. Okada, Y. Koyanagi, M. Kannagi, Y. Hinuma, *Science* **217**, 737 (1981); M. Popovic *et al.*, *ibid.* **219**, 856 (1983); I. S. Chen, S. G. Quan, D. W. Golde, *Proc. Natl. Acad. Sci. U.S.A.* **80**, 7006 (1983); M. Yoshida, M. Seiki, K. Yamaguchi, K. Takatsuki, *ibid.* **81**, 2534 (1984).
3. Y. Ito, *Curr. Topics Microbiol. Immunol.* **115**, 99 (1985).
4. R. C. Gallo, *Sci. Am.* **255**, 88 (December 1986); M. Ichimaru *et al.*, *Hematol. Oncol.* **4**, 21 (1986).
5. G. Franchini, F. Wong-Staal, R. Gallo, *Proc. Natl. Acad. Sci. U.S.A.* **81**, 6207 (1984).
6. Z. Salahuddin *et al.*, *Virology* **129**, 51 (1983).
7. J. A. Hoxie, D. M. Matthews, D. B. Cines, *Proc. Natl. Acad. Sci. U.S.A.* **81**, 7591 (1984); D. Ho, T. Rota, M. Hirsch, *ibid.*, p. 7588; K. Nagy, P. Clapham, R. Cheingsong-Popov, R. Weiss, *Int. J. Cancer* **32**, 321 (1983).
8. M. Popovic *et al.*, *Proc. Natl. Acad. Sci. U.S.A.* **80**, 5402 (1983).
9. P. Rodgers-Johnson *et al.*, *Lancet* **1985-II**, 1247 (1985); A. Gessain *et al.*, *ibid.*, p. 407; C. Bartholomew *et al.*, *ibid.* **1986-II**, 99 (1986); H. Koprowski *et al.*, *Nature (London)* **318**, 154 (1985).
10. S. Broder *et al.*, *Ann. Int. Med.* **100**, 543 (1984).
11. T. Kiyokawa *et al.*, *Gann.* **75**, 747 (1984); T. H. Lee *et al.*, *Science* **226**, 57 (1984); D. J. Slamon, K. Shimotohno, M. J. Cline, D. W. Golde, I. S. Y. Chen, *ibid.*, p. 61; W. A. Haseltine *et al.*, *ibid.* **225**, 419 (1984); W. C. Goh, J. Sodroski, C. A. Rosen, M. Essex, W. A. Haseltine, *ibid.* **227**, 1227 (1985); T. Kiyokawa, T. Kawaguchi, M. Seiki, M. Yoshida, *Virology* **147**, 462 (1985).
12. T. Kiyokawa *et al.*, *Proc. Natl. Acad. Sci. U.S.A.* **82**, 8359 (1985); K. Nagashima, M. Yoshida, M. Seiki, *J. Virol.* **60**, 394 (1986).
13. W. Wachsman *et al.*, *Science* **226**, 177 (1984); M. Seiki, A. Hikikoshi, T. Taniguchi, M. Yoshida, *ibid.* **228**, 1532 (1985).
14. J. G. Sodroski, C. A. Rosen, W. A. Haseltine, *ibid.* **225**, 381 (1984); J. Fujisawa, M. Seiki, T. Kiyokawa, M. Yoshida, *Proc. Natl. Acad. Sci. U.S.A.* **82**, 2277 (1985); B. K. Felber, H. Paskalis, C. Kleinman-Ewing, F. Wong-Staal, G. N. Pavlakis, *Science* **229**, 675 (1985); A. J. Cann *et al.*, *Nature (London)* **318**, 571 (1985).
15. W. Greene *et al.*, *Science* **232**, 877 (1986); J. Inoue *et al.*, *EMBO J.* **5**, 2883 (1986); M. Maruyama *et al.*, *Cell* **48**, 343 (1987).
16. J. M. Bishop, *Cell* **42**, 23 (1985).
17. W. S. Hayward, B. G. Neel, S. M. Astrin, *Nature (London)* **290**, 475 (1981).
18. M. Seiki, R. Eddy, T. B. Show, M. Yoshida, *ibid.* **309**, 640 (1984); M. Yoshida, M. Seiki, *Hematol. Oncol.* **4**, 13 (1986).
19. F. Wong-Staal *et al.*, *Nature (London)* **302**, 626 (1983); M. Seiki, S. Hattori, Y. Hirayama, M. Yoshida, *Proc. Natl. Acad. Sci. U.S.A.* **80**, 3618 (1983).
20. M. Hatanaka, *Hematol. Oncol.* **4**, 3 (1986).
21. V. Manzari *et al.*, *Proc. Natl. Acad. Sci. U.S.A.* **80**, 1574 (1983).
22. M. Kozak, *Nature (London)* **308**, 241 (1984).
23. C. A. Rosen *et al.*, *Proc. Natl. Acad. Sci. U.S.A.* **82**, 6502 (1985).
24. A. Gamallo *et al.*, *Physiol. Behav.* **36**, 835 (1986); J. N. Schwartz *et al.*, *Am. J. Pathol.* **79**, 509 (1975); T. F. Dougherty, *Physiol. Rev.* **32**, 379 (1952).
25. S. H. Hinrichs *et al.*, *Science* **237**, 1340 (1987).
26. E. Southern, *J. Mol. Biol.* **98**, 503 (1975).
27. T. Maniatis, E. F. Fritsch, J. Sambrook, *Molecular Cloning: A Laboratory Manual*, (Cold Spring Harbor Laboratory, Cold Spring Harbor, NY, 1982), p. 202.
28. H. Towbin, T. Staehelin, J. Gordon, *Proc. Natl. Acad. Sci. U.S.A.* **76**, 4350 (1979).
29. R. L. Brinster *et al.*, *ibid.* **82**, 4438 (1985).

30. We thank S. Oroszlan for providing the antibody to the tat protein, S. Josephs for clone pHX3 from which the *tat* coding sequence was derived, W. Haseltine for clone pU3Rcat from which the LTR sequence was obtained, and C. Bieberich, E. Jaffe, S. Nerenberg, A. Rabson, and J. Vogel for suggestions.

2 March 1987; accepted 21 July 1987